Excitation Function and Reaction Threshold Studies of Isotope Exchange Reactions: H + D_2 → D + HD and H + D_2O → D + HOD

Richard A. Brownsword, Matthias Hillenkamp, Thomas Laurent, Hans-Robert Volpp,* and Jürgen Wolfrum

Physikalisch-Chemisches Institut der Universität Heidelberg, Im Neuenheimer Feld 253, D-69120 Heidelberg, Germany

Rajesh K. Vatsa

Chemistry Division, Bhabha Atomic Research Centre, Bombay 400-085, India

Hee-Soo Yoo

Department of Chemistry, Chungbuk National University, Cheongju 361-763, Korea

Received: March 4, 1997; In Final Form: May 15, 1997[⊗]

Laser photolysis of H_2S at 248 nm and at 193 nm was used to generate nonequilibrium distributions of translationally energetic hydrogen atoms at high dilution in a flowing moderator gas (N_2 or Ar). The pulsed laser photolysis/laser-induced fluorescence "pump-and-probe" method allowed the measurement of the line shapes of the moderated H atom Doppler profiles as well as the concentrations of D atoms produced in the reactive collisions between the H atoms and D_2 or D_2O reagents. H and D atoms were detected with sub-Doppler resolution via ($2p^2P \leftarrow 1s^2S$) laser-induced fluorescence. The measured H atom Doppler profiles were used to describe the evolution of the initially generated nascent nonequilibrium H atom speed distribution toward its equilibrium Maxwell−Blotzmann form. In this way the excitation function and reaction threshold for the reactions H + D_2 → HD + D and H + D_2O → HOD + D could be determined for the first time from the measured nonequilibrium D atom formation rates and single-collision absolute reaction cross sections measured at higher collision energies.

I. Introduction

Soon after Born and Oppenheimer[1] in 1927 formulated in a precise manner the possibility of separating the electron from the nuclear motions, London,[2] in 1928, interpreted for the first time the elementary process of the exchange between a hydrogen atom and a hydrogen molecule in terms of a potential energy surface (PES). On the basis of the London approximation,[3] Eyring and Polanyi provided the first PES for the H + H_2 → H + H_2 chemical reaction.[4] This PES was later used for the first classical trajectory study[5] which, as early as in 1936, revealed the femtosecond nature of bimolecular reactive collisions, about 50 years before an experimental real-time study of a bimolecular reaction was reported by Bernstein, Zewail, and co-workers.[6]

Since then the H + H_2 reaction has become "the prototype test system" for the development of rigorous quantum mechanical atom−diatom scattering methods.[7,8] In the case of the H + H_2 reaction, it is the high accuracy of the available global PES representation[9] that ensures that comparison of the dynamical results with experiment indeed tests the theoretical method rather than the PES. About half a century after the first kinetics experiment carried out by Farkas,[10] experimental and theoretical results for the H + H_2 reaction were reviewed by Levine.[11] More recent reviews can be found in refs 12−14. The most recent advances in studying the reaction dynamics of the H + H_2 system include measurements of quantum state-specific differential cross sections[15−17] which allow for a very detailed comparison with quantum mechanical scattering calculations (QMS),[18] including those in which geometric phase effects were taken into account.[19]

In recent years, the H + H_2O ⇌ OH + H_2 reactions, as one of the "simplest" four-atom systems, have played an important role in the development of four-atom quantum reactive scattering methods.[20] For the reaction H + H_2O ⇌ H_2 + OH, absolute reaction cross sections were determined at different collision energies[21,22] allowing comparison with quasiclassical trajectory (QCT)[23] and with approximate[24,25] and accurate 6D-QMS calculations[26] on the Schatz−Elgersma (SE) PES.[27] References 28 and 29 provide an overview over the current experimental and theoretical status of the H + H_2O ⇌ H_2 + OH reactions.

Measurement of absolute reaction cross sections for the HD + OD and D_2 + OH product channels[30] of the partially isotopically substituted H + D_2O system at different collision energies confirmed that the reaction H + H_2O → H_2 + OH proceeds almost exclusively by a direct abstraction mechanism via a planar H−HOH transition state, rather than via the formation of a H_3O intermediate.[31] Only recently were dynamics studies of the exchange reaction H + D_2O → D + HOD carried out in our group,[32] in which it was found that at a collision energy of $E_{c.m.}$ = 2.2 eV, the reactive cross section for hydrogen exchange is considerably higher than the cross section for the hydrogen abstraction channel H + D_2O → HD + OD.[30b]

In the present article, we describe a moderated "hot" H atom pulsed laser "pump/probe" method which uses the photochemical technique of Kuppermann[33] for preparing energetic H atoms with known translational energies. This method is based on a combination of single collision reaction cross section,[34a] H atom moderation,[34b] and nonequilibrium D atom formation rate measurements. It allowed the determination of the reaction threshold and a global representation of the rotationally averaged

* To whom correspondence should be addressed.

[⊗] Abstract published in *Advance ACS Abstracts,* July 1, 1997.

S1089-5639(97)00816-5 CCC: $14.00

excitation function $\sigma_R(E_{c.m.})$ for both the three-atom $H + D_2 \rightarrow D + HD$ and the four-atom $H + D_2O \rightarrow D + HOD$ exchange reactions. For the $H + D_2$ reaction, the experimental results can be directly compared with recent 3D-QMS calculations on the Liu−Siegbahn−Truhlar−Horowitz (LSTH) PES by Charutz, Last, and Baer[35] which explicitly take into account the fact that the experimental results represent rotationally averaged quantities (averaged over the room temperature Boltzmann distribution of the D_2 rotational states). On the theoretical side, no dynamical study has so far been reported for the $H + D_2O \rightarrow D + HOD$ reaction. Only the $H' + H_2O \rightarrow H + H'OH$ hydrogen exchange reaction was investigated by Kudla and Schatz, who carried out QCT calculations on the SE-PES.[23b]

II. Experimental Section

The present experiments were carried out using the pulsed laser photolysis/laser-induced fluorescence "pump-and-probe" technique in a flow reactor system at room temperature. The apparatus and experimental method used in this study have been described in detail previously.[36,37] Hence, only details specific to the present investigation will be given in the following.

A. Experimental Setup and Conditions. The measurements were carried out in a flow reactor made of stainless steel, through which HX/D_2 (Messer Griesheim-MG, >99.7%) and HX/D_2O (Merck, D >99.95%) as H atom precursor/reagent mixtures together with a bath gas of N_2 (MG, 99.996%) or Ar (MG, 99.998%) could be continuously pumped through the reactor, with a flow rate high enough to ensure renewal of the gas mixture in the cell between successive photolysis ("pump") laser shots. H_2S (UCAR, electronic grade) and HCl (MG, > 99.999%) were used as H atom precursor compounds. The flow rates of H_2S, HCl, and D_2 were regulated by calibrated mass flow controllers; the D_2O flow was regulated using a glass valve. The cell pressure was measured by a MKS Baratron.

In the single collision absolute reaction cross section measurements, no bath gas was used. Typical values for the [HX]:[D_2] and [HX]:[D_2O] ratios were between 1:5 and 1:30. The experiments were carried out at low total pressure of $p_{tot} = 50-100$ mTorr and at short pump−probe delay times of $\Delta t = 80-180$ ns so as to avoid translational relaxation of the hot H atoms. The moderated hot H atom experiments were carried out for both reactions in an excess of N_2 and Ar buffer gas. In these experiments, the total pressure was typically 1−5 Torr with a HX/reagent partial pressure between 50 and 150 mTorr. H_2S, HCl, and D_2 partial pressures were determined from the flow rates while the D_2O partial pressure was measured using a photolytic calibration method similar to that used in ref 37. A number of test measurements were performed in order to find, for each reaction, suitable experimental conditions (such as type of moderator gas, HX/reagent ratios, and total pressure) in order to minimize such effects as secondary reaction of D atom products or fly-out of H atom reagents which might influence the results.

B. Generation of "Hot" H Atoms. Translationally "hot" H atoms with a nonequilibrium velocity distribution were generated by pulsed laser photolysis (with a laser pulse duration of about 15 ns) of the H atom precursors H_2S and HCl at different excimer laser wavelengths (248, 222, 193 nm). An aperture was used to skim off a homogeneous part of the rectangular excimer laser profile to provide a photolysis beam of about 3−7 mJ/pulse, which was slightly focused (focal length 1 m) and directed through the flow cell. At the photolysis laser intensities used in the present study, a linear dependence of the photolytically produced H atom concentrations on the intensity of the photolysis laser was observed and no secondary "high-energy" H atoms due to SH photolysis[38] were detectable. The 248 and 193 nm photodissociation laser (Lambda Physik, LPX 200) was operated without polarizing elements, and the analysis of the H atom Doppler profiles generated confirmed that the nascent velocity distributions were essentially spatially isotropic. The 222 nm photolysis laser (Lambda Physik, EMG 102 MSC) used in the single collision absolute reaction cross section measurements showed a preferential polarization. Due to the polarization of the photolysis laser beam, the H atom Doppler profile observed in the H_2S photolysis at 222 nm (see Figure 1b) exhibits a line shape characteristic of a perpendicular transition. The anisotropy of the H atom velocity distribution, however, does not affect the measurements of the total reaction cross section.

C. H Atom and D Atom Detection. H and D atoms were detected with sub-Doppler resolution via ($2p^2P \leftarrow 1s^2S$) laser-induced fluorescence using narrow-band ($\Delta\nu_{VUV} = 0.4$ cm^{-1}) VUV laser radiation generated using Wallenstein's method.[39] Laser radiation, tunable around the H (121.567 nm) and D (121.534 nm) atom Lyman-α transitions, was obtained by resonant third-order sum-difference frequency conversion ($\omega_{VUV} = 2\omega_R - \omega_T$) of pulsed dye laser radiation(pulse duration ~15 ns) in a phase-matched Kr−Ar mixture. The frequency ω_R ($\lambda_R = 212.55$ nm) was resonant with the Kr 4p−5p (1/2,0) two-photon transition while ω_T could be tuned from 844 to 848 nm to cover the H and D atom Lyman-α transitions. The generated Lyman-α light was carefully separated from the unconverted laser radiation by a lens monochromator. The VUV probe beam was aligned to overlap the photolysis beam at right angles in the viewing region of a laser-induced fluorescence (LIF) detector. The delay time between the photolysis and probe pulses was controlled by a pulse generator. The H and D LIF signal was measured through a band pass filter by a solar blind photomultiplier positioned at right angles to both photolysis and probe laser. Details of the background subtraction method used to remove small D atom signal contributions originating from D_2O photolysis by the probe laser are given in ref 32. The VUV-probe beam intensity was monitored after passing through the reaction cell with an additional solar blind photomultiplier. The LIF signal, VUV-probe beam intensity and the photolysis laser intensity were recorded with a boxcar system and transferred to a microcomputer where the LIF signal was normalized to both photolysis and probe laser intensities. In order to obtain a satisfactory signal to noise (S/N) ratio, each point of the H and D atom Doppler profiles (Figure 1) was averaged over 30 laser shots. Measurements were carried out at a repetition rate of 6 Hz.

III. Results

A. Single Collision Absolute Reaction Cross Sections. Absolute reaction cross sections at single collision energies were obtained using a pulsed laser pump/probe method as introduced by Bersohn and co-workers to measure absolute reaction cross sections for the $H + D_2$/HD hydrogen exchange reactions.[34a] Following ref 34a, the determination of the absolute reactive cross section σ_R for the $H + D_2 \rightarrow D + HD$ reaction, for example, is based on the following expression:

$$\sigma_R(E_{c.m.}) = S_D/(S_H v_{rel} [D_2] \Delta t) \quad (1)$$

v_{rel} is the relative velocity, $E_{c.m.} = {}^1/_2\mu v_{rel}^2$ stands for the corresponding average center-of-mass collision energy of the reactants, and μ is the reduced mass of the H−D_2 collision pair. $E_{c.m.}$, and hence v_{rel}, can be calculated from the photolysis laser wavelength, the H−X bond dissociation energy of the hot H

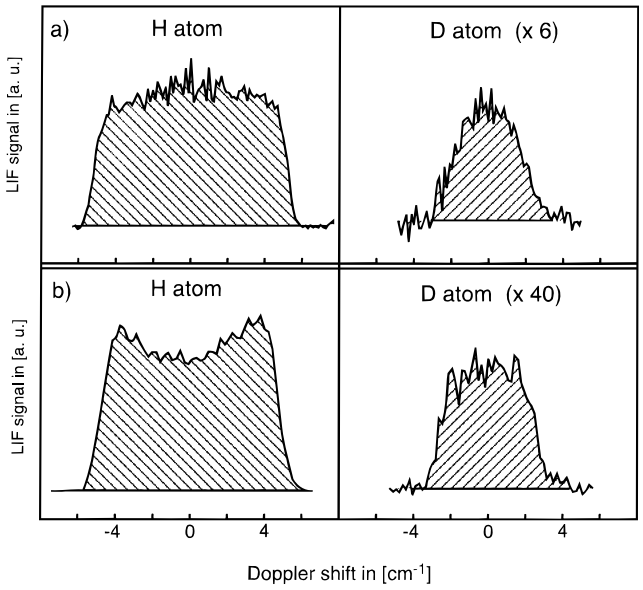

Figure 1. H atom reagent and D atom product Doppler profiles as obtained in the single collision reaction cross section studies: (a) The $H + D_2 \rightarrow D + HD$ reaction at $E_{c.m.} = 1.6$ eV. H atoms are generated via HCl photolysis at 193 nm in the presence of 55 mTorr D_2. (b) The $H + D_2O \rightarrow D + HOD$ reaction at $E_{c.m.} = 1.5$ eV. H atoms are generated via H_2S photolysis at 222 nm in the presence of 63 mTorr D_2O. In both cases D atom products are probed at a delay time of 130 ns. The centers of the LIF spectra correspond to the Lyman-α transition of the H (82 259.1 cm^{-1}) and D atom (82 281.4 cm^{-1}), respectively.

atom precursor molecule, and the internal state distribution of the X fragment, as described in detail in ref 40. Δt is the time delay between pump and probe laser pulses, which was determined by measuring the time difference between photolysis and probe scattered light pulses observed on a fast oscilloscope. $[D_2]$ denotes the concentration of the D_2 reagent present in excess, which is therefore essentially constant. S_D and S_H are the integrated areas of the corresponding Doppler profiles (see Figure 1), which are a measure of the relative concentrations of the photolytically produced H atom reagent $[H]_{\Delta t=0}$ and the D atom reaction products $[D]_{\Delta t}$. A more detailed description of the single collision reactive cross section measurement method can be found in ref 34a.

Figure 1a shows H atom and D atom profiles observed when a room-temperature mixture of HCl and D_2 was irradiated by laser light with a wavelength of 193 nm. H and D atom profiles observed after irradiation of a room-temperature mixture of H_2S and D_2O laser light with a wavelength of 222 nm are depicted in Figure 1b. For the reactions $H + D_2$ and $H + D_2O$, the average collision energies are 1.6 and 1.5 eV, respectively. In the latter measurements, a small D atom background was observed, originating from the direct photolysis of D_2S/HDS believed to be formed by fast heterogenous isotope exchange between H_2S and D_2O at the walls of the flow system. The D atom profile shown in Figure 1b has been corrected for this background and therefore represents D atoms solely produced by the gas phase reaction of H atoms with D_2O. Details of the experimental background correction procedure for the measurements of absolute reaction cross section for the $H + D_2O$ hydrogen exchange are given in ref 32. When HCl/D_2 or H_2S/D_2 mixtures were flowing through the cell, no such photolytic D atom background was observed. This D atom background was also absent when flowing mixtures of H_2S and D_2O diluted in a large excess of buffer gas were photolyzed, as described in the next section.

For the $H + D_2 \rightarrow D + HD$ reaction, the following absolute reaction cross sections were measured

$$\sigma_R(0.9\ \text{eV}) = 0.97 \pm 0.11\ \text{Å}^2$$

$$\sigma_R(1.6\ \text{eV}) = 1.23 \pm 0.32\ \text{Å}^2$$

$$\sigma_R(2.0\ \text{eV}) = 1.28 \pm 0.28\ \text{Å}^2$$

and found to be in excellent agreement with the earlier results by Bersohn and co-workers (see ref 34a, Table 1). H atoms with collision energies of 0.9 and 2.0 eV were generated by the photolysis of H_2S at a wavelength of 248 and 193 nm, respectively.

For the $H + D_2O \rightarrow D + HOD$ reaction, for which an absolute reactive cross section of $\sigma_R(2.2\ \text{eV}) = 0.36 \pm 0.15\ \text{Å}^2$ was recently measured,[32] the following value was obtained at a collision energy of $E_{c.m.} = 1.5$ eV:

$$\sigma_R(1.5\ \text{eV}) = 0.26 \pm 0.06\ \text{Å}^2$$

B. Moderated Hot H Atom Experiments. Principle. When translationally hot H atoms are generated by pulsed laser photolysis of HX-type precursor molecules in a large excess of a moderator gas, the initially present nascent nonequilibrium H atom velocity distribution[40] evolves toward the thermal equilibrium distribution determined by the temperature of the moderator gas, which under these conditions acts as a heat bath. In this case the velocity distribution of the H atoms in the laboratory frame has to be described by a time-dependent distribution function $f(v_{rel},t)$ for which the time evolution is given by a linearized Boltzmann equation.[34b] When, in addition, a reagent is present, reactive collisions occur in competition with the translational relaxation. The nonequilibrium kinetics—for example the formation of D atoms in the moderated hot H atom reaction $H + D_2 \rightarrow D + HD$—are then described by the following rate equation:

$$\frac{d[D]_t}{dt} = \{\int_0^\infty \sigma_R(v_{rel}) v_{rel} f(v_{rel},t)\, dv_{rel}\}[H]_t[D_2] \qquad (2)$$

Here it has been assumed that D_2 is present in excess over H atoms so that the D_2 concentration remains constant in time. The term in braces represents the reaction rate constant which, under the translationally nonequilibrium conditions of the present experiments, is time-dependent. After $[H]_t$ is replaced by $[H]_{t=0} - [D]_t$ and the new variable $\chi_D(t) = [D]_t/[H]_{t=0}$ is introduced—representing the fractional yield of D atoms produced—the following expression

$$\chi_D(\Delta t) = [D_2] \int_0^{\Delta t} \{\int_0^\infty \sigma_R(v_{rel}) v_{rel} f(v_{rel},t)\, dv_{rel}\}(1 - \chi_D(t))\, dt \qquad (3)$$

can be obtained as a solution of eq 2 for the initial condition $\chi_D(t=0) = 0$. The delay time Δt between the pump laser pulse, which generates the H atom reagents, and the probe laser pulse, which detects the D atom products, corresponds to the reaction time. In order to perform the integration in eq 3, one has to know the excitation function, i.e., the reaction cross section σ_R as a function of the relative velocity, as well as the time dependence of the relative velocity distribution function $f(v_{rel},t)$. On the other hand, when $\chi_D(\Delta t)$ and $f(v_{rel},t)$ can be measured, information about the actual form of the excitation function can be obtained.

Experimental Realization and Data Analysis. The experimental method used in the present studies allowed the direct determination of both the D atom product yield $\chi_D(\Delta t)$ and the time dependent relative velocity distribution function $f(v_{rel},t)$.

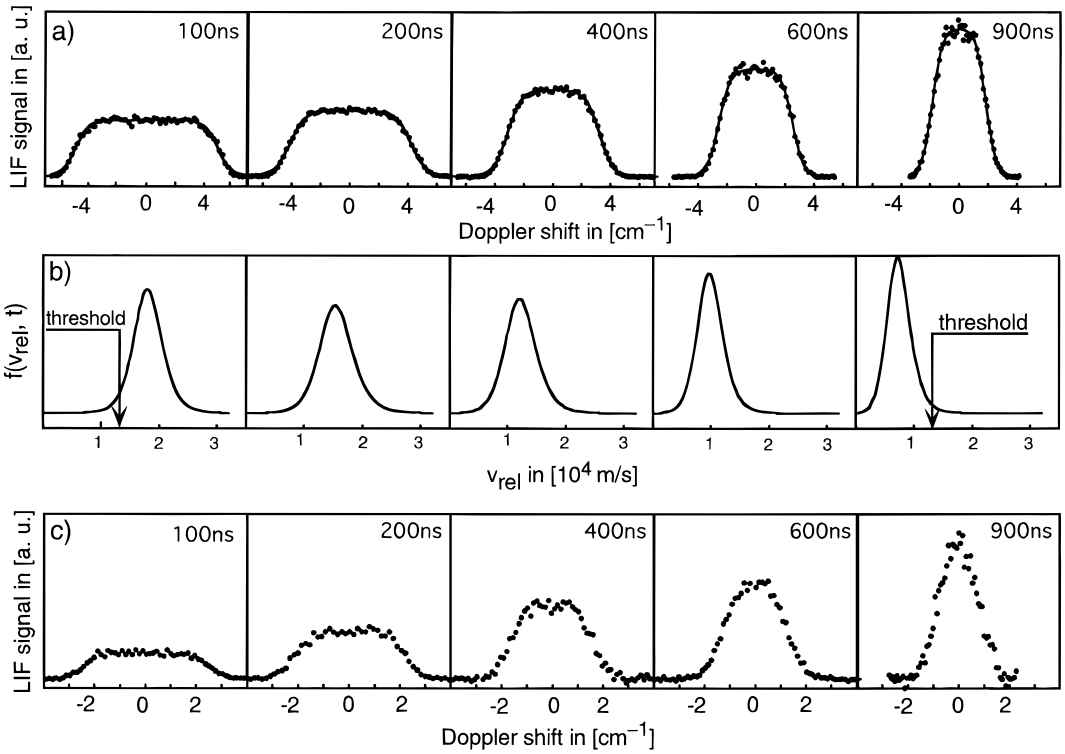

Figure 2. (a) H atom Doppler profiles measured at different pump/probe delay times between 100 and 900 ns after 193 nm photolysis of H_2S in a flowing mixture of 120 mTorr D_2O and 1.4 Torr Ar. Solid lines are results of a fit to the time evolution of H atom laboratory velocity distribution $f(v_z,t)$ as described in the text. (b) Evolution of the corresponding time-dependent distribution function $f(v_{rel},t)$ of the relative velocity of the H−D_2O reagents. The arrows mark the threshold for the H + D_2O → D + HOD reaction. (c) Doppler profiles of D atoms produced in the reaction. The D atom signal after 900 ns corresponds to a D atom product yield of $\chi_D(900\text{ ns}) = [D]_{900ns}/[H]_{t=0} = 0.054$.

$\chi_D(\Delta t)$ was obtained by calculating the ratio of the integrated areas of the D atom product measured at reaction time Δt (see, e.g., Figure 2) and the nascent H atom reagent Doppler profile measured at a reaction time close to zero (before significant reaction could occur).

If, as in the case of the present experiments, collisional and radiative lifetime broadening are negligible, an H atom Doppler profile measured at a given time t (see Figure 2a) directly reflects, via the linear Doppler shift $\nu - \nu_0 = v_z\nu_0/c$, the laboratory frame distribution $f(v_z,t)$ of the velocity component v_z of the absorbing atoms along the propagation direction of the probe laser beam. Therefore the evaluation of H atom Doppler line shapes measured at different pump/probe delay times allows the time evolution of the v_z velocity component $f(v_z,t)$ to be derived. In the present study a symmetric double sigmoidal function, eq 4,

$$f(v_z,t) = A_0\left[\frac{1}{1+\exp\left\{-\dfrac{(v_z+\omega_1/2)}{\omega_2}\right\}}\right]\left[1-\frac{1}{1+\exp\left\{-\dfrac{(v_z-\omega_1/2)}{\omega_2}\right\}}\right] \quad (4)$$

was used as a fitting function to evaluate the measured Doppler line shape, as it well describes the Doppler line shapes at both short and long pump−probe delay times (see Figure 2a). In eq 4, A_0 is a normalization factor, while the two variables ω_1 and ω_2 are a measure for the width of the profile and the steepness of its wings, respectively. In order to derive an empirical representation of $f(v_z,t)$, ω_1, and ω_2 were parameterized by the following time-dependent expressions:

$$\omega_1(t) = a_1 + b_1\exp(-c_1t) \quad (5)$$

$$\omega_2(t) = a_2 + b_2\exp\left\{-\left(\frac{t-c_2}{d_2}\right)^2\right\} \quad (6)$$

In Figure 3, the solid lines represent the results of a least-squares fit of the measured data which was used to determine the functional form of $\omega_1(t)$ and $\omega_2(t)$ under the conditions of the moderated hot H atom experiments. If the H atom velocity distribution function is known to be isotropic, $f(v_{rel},t)$ can be easily obtained, by differentiation of $f(v_z,t)$ followed by a laboratory to center-of-mass transformation, as described in detail in refs 34b and 40. It has been shown[34b] that in the present case of moderation of H atoms by Ar, any initial anisotropy of the H atom velocity distribution created by the laser photolysis of H_2S[41] decays rapidly (within a few collisions) compared to the H atom kinetic energy. In the present experiments, the H atom velocity distribution was found to be isotropic even at the shortest reaction times Δt.

In Figure 2a, H atom Doppler profiles (represented by the solid lines), simulated using eq 4 as the empirical representation of $f(v_z,t)$, are depicted and compared to the experimental ones (solid circles). In Figure 2b, the corresponding time-dependent distribution function $f(v_{rel},t)$ obtained from $f(v_z,t)$ is depicted. Doppler profiles of the D atoms produced are shown in Figure 2c. The reaction time at which the H and D atoms were detected are given in the figure.

Typical examples of measured D atom fractional yields, $\chi_D(\Delta t)$, are shown in Figure 4 for the reactions H + D_2 → D + HD and H + D_2O → D + HOD. The experimental data were analyzed by assuming a suitable form for the excitation function $\sigma_R(v_{rel})$—such as the simple "line-of-centers" (LOC) function[42]—containing parameters (such as the threshold energy E_0 for reaction) to be optimized. Using the time-dependent param-

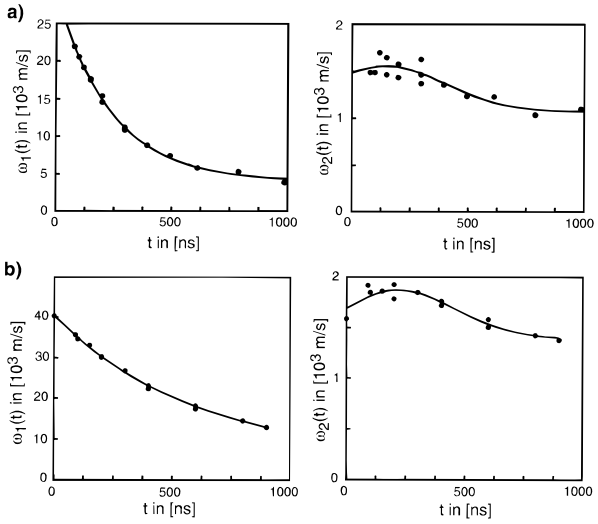

Figure 3. Measured time-dependence of the H atom line shape parameters ω_1 and ω_2 (solid circles): (a) 248 nm H_2S photolysis in a flowing mixture of 100 mTorr D_2 and 1.1 Torr N_2; (b) 193 nm H_2S photolysis in a flowing mixture of 120 mTorr D_2 and 1.4 Torr Ar. Solid lines are the results of a least-squares fit procedure used to derive a continuous analytical representation for the two parameters $\omega_1(t)$ and $\omega_2(t)$.

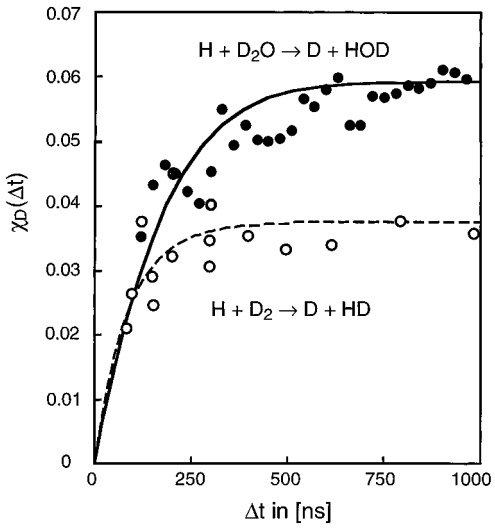

Figure 4. Plots of D atom product yields χ_D versus reaction time. Symbols (○) and (●) represent experimental results. The dashed and solid lines are results of simulations of the experimental moderation conditions using the excitation functions $\sigma_R(E_{c.m.})$ shown in Figure 5a and Figure 5b for the H + D_2 → D + HD and H + D_2O → D + HOD reaction, respectively, and the measured velocity distributions $f(v_{rel},t)$.

eterization of the H atom speed distribution $f(v_{rel},t)$ determined for each set of experimental conditions, D atom fractional yields predicted by the model excitation function could be calculated (e.g., dashed and solid lines in Figure 4), via eq 3, for the conditions corresponding to each measured data point $\chi_D(\Delta t)$. The integration over t in eq 3 was performed numerically, using a fourth-order Runge−Kutta algorithm incorporating error and adaptive step-size control.[43] A measure of the quality of a given set of excitation function parameters was obtained by computing the global mean squared deviation of both the nonequilibrium kinetics data sets and the single collision cross sections from the corresponding values calculated from the trial excitation function. Optimization of the excitation function parameters was performed by a nonlinear least-squares fit to minimize the sum of these two mean squared deviations.

H + D_2 → D + HD. For both the H + D_2 and H + D_2O reaction, the LOC excitation function was tried as an initial model function. In the case of the reaction H + D_2, however, it proved not possible to find a set of parameters in the framework of a LOC model which provided a good description of both the nonequilibrium kinetics and the single-collision data sets. As the excitation function at high collision energies (1.6 eV ≤ $E_{c.m.}$ ≤ 2.7 eV) is already reasonably well-characterized by the single collision cross section measured in the present work and in ref 34b, the excitation function given by eq 7 was tested.

$$\sigma_R(E_{c.m.}) = \begin{cases} \dfrac{1.52}{1+\exp\left\{-\dfrac{(E_{c.m.}-\epsilon)}{\eta}\right\}} - 0.25 & \text{for } E_{c.m.} \geq E_0 \\ 0 & \text{for } E_{c.m.} < E_0 \end{cases} \quad (7)$$

This form of the excitation function is arbitrary but ensures that the cross section reaches asymptotically a constant value of $\bar{\sigma}_R$ = 1.26 Å^2 for $E_{c.m.}$ ≥ 1.6 eV. $\bar{\sigma}_R$ represents the average value of the single collision cross sections measured in the present work and in ref 34b at collision energies of $E_{c.m.}$ = 1.6, 2.0, and 2.7 eV. The model parameters ϵ and η determine the position of the reaction threshold energy and the steepness of the rise of the function below 1.6 eV. The aim of this approach was to obtain information about the reaction cross section in the less well-characterized region below $E_{c.m.}$ = 1.6 eV. The two parameters were optimized as described above to yield the excitation function shown in Figure 5a, which corresponds to a reaction threshold energy of E_0 = 0.40 ± 0.14 eV (1σ). The statistical uncertainty in each of the model parameters ϵ and η allows the confidence region (1σ) of the excitation function to be estimated[43] and is shown as the shaded area in Figure 5a.

H + D_2O → D + HOD. In the case of the H + D_2O → D + HOD reaction, the LOC model was able to reproduce adequately both the nonequilibrium kinetic and the single collision measurements of the present work at $E_{c.m.}$ = 1.5 eV and of ref 32 at $E_{c.m.}$ = 2.2 eV. No systematic deviation between measured and simulated data was observed that would justify the use of a more flexible or sophisticated excitation function. The optimized parameters for the LOC excitation function

$$\sigma_R(E_{c.m.}) = \begin{cases} \sigma_0\left(1-\dfrac{E_0}{E_{c.m.}}\right) & \text{for } E_{c.m.} \geq E_0 \\ 0 & \text{for } E_{c.m.} < E_0 \end{cases} \quad (8)$$

are E_0 = 0.88 ± 0.11 eV and σ_0 = 0.62 ± 0.09 Å^2 (both errors 1σ). This function, together with the 1σ confidence region, is depicted in Figure 5b.

IV. Discussion

H + D_2 → D + HD. In Figure 5a, the global excitation function derived in the present study is depicted. Single collision reaction cross sections obtained in the present study and by Bersohn and co-workers,[34a] who used an identical experimental method and comparable experimental conditions, are also shown. The experimental uncertainties of the present experiment are comparable (see section III.A) to those of ref 34a and are for reasons of clarity not depicted in Figure 5a. The single collision reaction cross sections σ_R (1.6 eV) and σ_R (2.0 eV) measured in the present study are in excellent agreement with the earlier Bersohn values[34a] and clearly confirm the results of the early QCT calculations by Schechter, Kosloff and Levine[44] on the LSTH-PES, who found that the excitation function shows a broad maximum of ∼1.3 Å^2 around $E_{c.m.}$ ≈ 2

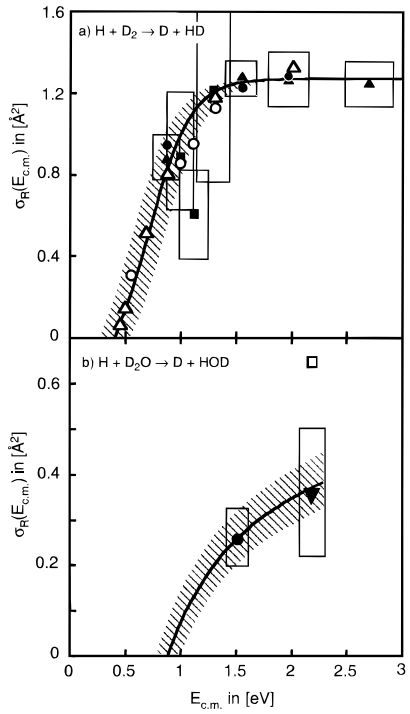

Figure 5. Comparison between theoretical and experimental reaction cross sections. All experimental results represent rotationally averaged values (averaged over the room temperature D_2/D_2O reagent rotational state distribution). The solid lines are the excitation functions $\sigma_R(E_{c.m.})$ as derived in the present study. The shaded area reflects the statistical uncertainty (1σ) of the global least-squares fit procedure used to determine the optimum excitation function (for details see text). In (a) the symbols (■), (▲), and (●) are experimental single collision reaction cross sections from refs 12 and 34a and from the present study, respectively. (○) and (△) are rotationally averaged cross sections obtained in QCT (ref 49) and in recent 3D-QMS (ref 35) calculations on the LSTH-PES. In (b) the symbols (●) and (▼) are experimental single collision reaction cross sections from our previous study (ref 32) and from the present study. (□) is the result of a QCT calculation (ref 23b) for the H′ + H_2O → H + H′OH exchange reaction carried out on the SE-PES. The width of the boxes drawn around the single collision cross sections represents the spread (fwhm) in the collision energy distribution and the height of the boxes represents the experimental uncertainties in the measurements.

eV. The assumption $\sigma_R(E_{c.m.}) = \bar{\sigma}_R = 1.26$ Å^2 for 1.6 eV ≤ $E_{c.m.} \leq 2.7$ eV made in the construction of the global excitation function (eq 7) for the H + D_2 reaction is therefore definitely justified. A discussion of the validity of previous cross section measurements at collision energies around 2 eV,[45] which yielded considerably higher values, is given in ref 12.

Absolute reaction cross sections by Valentini and coworkers[12] are also included in Figure 5a as filled squares. These reaction cross sections were determined by summation over partial cross sections for HD(v,J) formation, measured using coherent anti-Stokes Raman scattering (CARS) spectroscopy. While the values obtained at $E_{c.m.} = 1$ and 1.3 eV are in line with the present results, the cross section at $E_{c.m.} = 1.1$ eV is considerably lower. The dispute concerning the suggestion[12] that the appearance of this rather low value might originate from a dynamical resonance[46] in the excitation function has finally been settled against this suggestion.[47] It seems that the scatter of this value simply reflects the higher experimental uncertainty in the CARS measurements, originating from the fact that the HD product to be detected is formed with an internal state distribution covering a number of vibrational and a wide range of rotational states.[12,48]

In Figure 5a, comparison is made between the global excitation function obtained in the present study and QCT[49] and 3D-QMS[35] reaction cross sections calculated using the LSTH-PES. The theoretical reaction cross sections represent rotationally averaged quantities; in order to account explicitly for the experimental conditions the reactive cross sections were averaged over a room temperature Boltzmann distribution of the D_2 rotational states. So both the quasiclassical and the quantum mechanical cross sections can be directly compared with the experimental results. Therefore any difference regarding the agreement with experiment can be attributed directly to the type of theoretical concept used in the calculations. The fact that the QMS results show in general a somewhat better agreement with experiment clearly favors—even at collision energies as high as 2 eV—the quantum mechanical reactive scattering approach over the classical one.

H + D_2O → D + HOD. In Figure 5b, the LOC excitation function as determined in the present study for the H + D_2O → D + HOD reaction is depicted together with the two available single collision reaction cross sections. The experimental uncertainty of the single collision reaction cross section measured at $E_{c.m.} = 2.2$ eV is—for reasons described in detail in ref 32—markedly higher than in the corresponging H + D_2 experiments. A comparison can be made between the present study and an earlier experiment by Bibler and Firestone[50] who determined hydrogen exchange yields after irradiating gaseous TOD−D_2O−H_2 mixtures with β-particles. In ref 50, a probable activation energy of 19.1 ± 0.5 kcal/mol (0.83 ± 0.02 eV) was suggested for the H + D_2O → D + HOD reaction, which is consistent with the room temperature average reaction threshold energy of 0.88 ± 0.11 eV as obtained in the present work.

So far only one theoretical dynamical study has been reported by Kudla and Schatz[23b] who carried out QCT calculations on the SE-PES to determine an absolute reaction cross section (see Figure 5b) for the exchange reaction H′ + H_2O → H + H′OH at a collision energy of $E_{c.m.} = 2.2$ eV. In comparison with experimental results it should be noted that the transition state for the hydrogen exchange reaction might be represented in the SE-PES with only minor accuracy, because none of its properties were actually optimized in developing the global fit. Therefore the significantly higher QCT cross section either could originate from the presence of a real isotope effect or could be due to the inaccuracy of the PES employed. The latter explanation might be favored by *ab initio* calculations of low-lying H_3O states[31] in which a classical barrier height of 0.93 eV for the H′ + H_2O → H + H′OH hydrogen exchange reaction was determined. This value is considerably higher than that of the corresponding barrier of about 0.41 eV on the SE-PES. For an assessment of the global accuracy of both the SE-PES and the newly developed Kliesch−Werner−Clary-PES,[29b] extended QCT studies of the H + D_2O → D + HOD reaction covering the energy range of the present study would be helpful. However, the most rigorous comparison between theory and experiment definitely requires the application of QMS methods to the H + D_2O multichannel reaction system.

V. Summary

A new experimental method was applied to determine rotationally averaged reaction thresholds and information about the excitation functions of the H + D_2 → D + HD triatomic and the H + D_2O → D + HOD tetraatomic isotope exchange reactions from a combination of single collision cross section measurements and moderated hot H atom experiments. The global representations of the excitation functions derived in the present study best describe the currently available experimental reaction cross section data over a wide range of collision energies. For the H + D_2 archetypes system a very good

agreement between the experimental excitation function and the most recent 3D-QMS reaction cross section calculations on the LSTH-PES was obtained. The present results represent the first measurement of the reaction threshold and the excitation function for the exchange reaction $H + D_2O \rightarrow D + HOD$. For this reaction, much less theoretical dynamical information is available so far. The experimental data presented in this study can serve as a reference in the development of a more accurate global PES as well as in the development of approximate and accurate quantum mechanical methods for the treatment of four-atom multichannel reactions.

Acknowledgment. The authors gratefully acknowledge financial support of the Deutsche Forschungsgemeinschaft and the Alexander von Humboldt Stiftung. R.K.V. wishes to acknowledge a fellowship provided by the KFA Jülich and DLR Bonn under the Indo-German bilateral agreement (Project CHEM-19). H.S.Y. acknowledges support from the Center for Molecular Science at the Korea Advanced Institute of Science and Technology (KAIST, Korea). H.R.V. wishes to thank G. C. Schatz for helpful comments during the preparation of the manuscript, Dr. M. Mladenovic for communicating interesting details about dynamical resonances, and M. Baer for stimulating discussions about the quantum mechanical treatment of atom exchange reactions. The collaboration with M. Baer was made possible by a grant (No. E1447) from the Bundesministerium für Bildung und Forschung (BMBF, Germany).

References and Notes

(1) Born, M.; Oppenheimer, J. R. *Ann. Phys.* **1927**, *84*, 451.

(2) London, F. *Sommerfeldfestschrift*; Hirzel: Leipzig, 1928.

(3) London, F. *Z. Elektrochem.* **1929**, *35*, 552.

(4) Eyring, H.; Polanyi, M. *Z. Phys. Chem.* **1931**, *B12*, 279.

(5) Hirschfelder, J. O.; Eyring, H.; Topley, B. *J. Chem. Phys.* **1936**, *4*, 170.

(6) Scherer, N. F.; Khundkar, L. R.; Bernstein, R. B.; Zewail, A. H. *J. Chem. Phys.* **1987**, *82*, 1451.

(7) See, e.g.: (a) Truhlar, D. G.; Wyatt, R. E. *Annu. Rev. Phys. Chem.* **1976**, *27*, 1. (b) Baer, M. *Theory of Chemical Reaction Dynamics, Vol I−IV*; CRC Press: Boca Raton, 1985. (d) Schatz, G. C. In *The Theory of Chemical Reaction Dynamics*; Clary, D. C., Ed.; Reidel: Dordrecht, 1986.

(8) For a recent review see: Schatz, G. C. *J. Phys. Chem.* **1996**, *100*, 12839.

(9) Liu, B. *J. Chem. Phys.* **1973**, *58*, 1925. Siegbahn, P.; Liu, B. *J. Chem. Phys.* **1978**, *68*, 2457. Truhlar, D. G.; Horowitz, C. J. *J. Chem. Phys.* **1978**, *68*, 2466. *J. Chem. Phys.* **1979**, *71*, 1514.

(10) Farkas, A. *Z. Phys. Chem.* **1930**, *B10*, 419.

(11) Levine, R. D. The Farkas Memorial Symposium: Fifty Years of $H + H_2$ Kinetics. *Int. J. Chem. Kinet.* **1986**, *18*, 9.

(12) Valentini, J. J.; Phillips, D. L. In *Advances in Gas Phase Photochemistry and Kinetics, Vol. 2*; Ashfold, M. N. R., Baggott, J. E., Eds.; Royal Society of Chemistry: London, 1989.

(13) Buchenau, H.; Toennies, J. P.; Arnold, J.; Wolfrum, J. *Ber. Bunsenges. Phys. Chem.* **1990**, *94*, 1231.

(14) Michael, J. V. In *Advances in Chemical Kinetics and Dynamics, Vol. 1*; Barker, R., Ed.; JAI Press: Greenwich, 1992.

(15) Continetti, R. E.; Balko, B. A.; Lee, Y. T. *J. Chem. Phys.* **1990**, *93*, 5719.

(16) Kitsopoulos, T. N.; Buntine, M. A.; Baldwin, D. P.; Zare, R. N.; Chandler, D. W. *Science* **1993**, *262*, 1852.

(17) Schnieder, L.; Seekamp-Rahn, K.; Liedeke, F.; Steuwe, H.; Welge, K. H. *Faraday Discuss. Chem. Soc.* **1991**, *9*, 259. Schnieder, L.; Seekamp-Rahn, K.; Borkowski, J.; Wrede, E.; Welge, K. H.; Aoiz, F. J.; Bañares, L.; D'Mello, M. J.; Herrero, V. J.; Sáez Rábanos, V.; Wyatt, R. E. *Science* **1995**, *269*, 207. Wrede, E.; Schnieder, L.; Welge, K. H.; Aoiz, F. J.; Bañares, L.; Herrero, V. J. *Chem. Phys. Lett.* **1997**, *265*, 129.

(18) D'Mello, M. J.; Manolopoulos, D. E.; Wyatt, R. E. *Science* **1994**, *263*, 102.

(19) Wu, Y.-S.; Kuppermann, A. *Chem. Phys. Lett.* **1993**, *205*, 577; **1993**, *213*, 636; **1995**, *255*, 105.

(20) (a) Miller, W. H. *Annu. Rev. Phys. Chem.* **1990**, *41*, 245; *Acc. Chem. Res.* **1993**, *26*, 174. (b) Sun, Q.; Bowman, J. M. *J. Chem. Phys.* **1990**, *92*, 5201. (c) Clary, D. C. *J. Chem. Phys.* **1991**, *95*, 7298. (d) Zhang, D. H.; Zhang, J. Z. H. *J. Chem. Phys.* **1993**, *99*, 5615; **1994**, *100*, 2679; **1994**, *101*, 5615. (e) Manthe, U.; Seideman, T.; Miller, W. H. *J. Chem. Phys.* **1993**, *99*, 10078; **1994**, *101*, 4759. (f) Neuhauser, D. *J. Chem. Phys.* **1994**, *100*, 9272. (g) Balakrishnan, N.; Billing, G. D. *Chem. Phys.* **1994**, *101*, 2785; **1995**, *102*, 1102. (h) Szichman, H.; Baer, M. *Chem. Phys. Lett.* **1995**, *242*, 285.

(21) Kleinermanns, K.; Wolfrum, J. *Appl. Phys. B* **1984**, *34*, 5. Kessler, K.; Kleinermanns, K. *Chem. Phys. Lett.* **1992**, *190*, 145.

(22) Jacobs, A.; Volpp, H.-R.; Wolfrum, J. *24th Symp. (Int.) on Combustion*; The Combustion Institute: Pittsburgh, PA, 1992; p 605; *Chem. Phys. Lett.* **1992**, *196*, 249; **1994**, *218*, 51; *J. Chem. Phys.* **1994**, *100*, 1936.

(23) (a) Schatz, G. C.; Colton, J. L.; Grant, M. C. *J. Phys. Chem.* **1984**, *88*, 2971. (b) Kudla, K.; Schatz, G. C. *J. Chem. Phys.* **1993**, *98*, 4644.

(24) Nyman, G.; Clary, D. C. *J. Chem. Phys.* **1994**, *100*, 3556.

(25) Baer, M.; Szichman, H.; Rosenman, E.; Hochman-Kowal, S.; Persky, A. In *Gas Phase Chemical Reaction Systems: Experiments and Models 100 Years after Max Bodenstein*; Wolfrum, J., Volpp, H.-R., Rannacher, R., Warnatz, J., Eds.; Springer Series in Chemical Physics Vol. 61; Springer-Verlag: Heidelberg, 1996.

(26) Zhang, D. H.; Light, J. C. *J. Chem. Phys.* **1996**, *104*, 4544.

(27) Schatz, G. C.; Elgersma, H. *Chem. Phys. Lett.* **1980**, *73*, 21.

(28) Crim, F. F. *J. Phys. Chem.* **1996**, *100*, 12725.

(29) (a) Schatz, G. C.; Bowman, J. M. *Annu. Rev. Phys. Chem.* **1995**, *46*, 169. (b) Alagia, M.; Balucani, N.; Casavecchia, P.; Stranges, D.; Volpi, G. G.; Clary, D. C.; Kliesch, A.; Werner, H.-J. *Chem. Phys.* **1996**, *207*, 389.

(30) (a) Jacobs, A.; Volpp, H.-R.; Wolfrum, J. *Chem. Phys. Lett.* **1992**, *196*, 249. (b) Koppe, S.; Laurent, T.; Naik, P. D.; Volpp, H.-R.; Wolfrum, J. *Can. J. Chem.* **1994**, *72*, 614 Paper dedicated to Professor J. C. Polanyi on the occasion of his 65th birthday.

(31) Talbi, D.; Saxon, R. *J. Chem. Phys.* **1989**, *91*, 2376.

(32) Brownsword, R. A.; Hillenkamp, M.; Laurent, T.; Vatsa, R. K.; Volpp, H.-R.; Wolfrum, J. *Chem. Phys. Lett.* **1996**, *259*, 375.

(33) Kuppermann, A. *Isr. J. Chem.* **1969**, *7*, 303.

(34) (a) Johnston, G. W.; Katz, B.; Tsukiyama, K.; Bersohn, R. *J. Phys. Chem.* **1987**, *91*, 5445. (b) Park, J.; Shafer, N.; Bersohn, R. *J. Chem. Phys.* **1989**, *91*, 7861.

(35) Charutz, D. M.; Last, I.; Baer, M. *J. Chem. Phys.* **1997**, *106*, 7654.

(36) Laurent, T.; Naik, P. D.; Volpp, H.-R.; Wolfrum, J.; Arusi-Parpar, T.; Bar, I.; Rosenwaks, S. *Chem. Phys. Lett.* **1995**, *236*, 343. Brownsword, R. A.; Hillenkamp, M.; Laurent, T.; Vatsa, R. K.; Volpp, H.-R. *J. Chem. Phys.* **1997**, *106*, 4436.

(37) Brownsword, R. A.; Hillenkamp, M.; Laurent, T.; Vatsa, R. K.; Volpp, H.-R.; Wolfrum, J. *J. Phys. Chem.* **1997**, *101*, 995.

(38) Continetti, R. E.; Balko, B. A.; Lee, Y. T. *Chem. Phys. Lett.* **1991**, *182*, 400.

(39) Hilber, G.; Lago, A.; Wallenstein, R. *J. Opt. Soc. Am. B* **1987**, *4*, 1753.

(40) Zande, W. J. v. d.; Zhang, R.; Zare, R. N.; McKendrick, K. G.; Valentini, J. J. *J. Phys. Chem.* **1991**, *95*, 8205.

(41) van Veen, G. N. A.; Mohamed, K. A.; Baller, T.; de Vries, A. E. *Chem. Phys.* **1983**, *74*, 261.

(42) Levine, R. D.; Bernstein, R. B. *J. Chem. Phys.* **1972**, *56*, 2281.

(43) Press, C. W. H.; Flannery, B. P.; Teukolsky, S. A.; Vetterling, W. T. *Numerical Recipes in C*; Cambridge University Press: Cambridge, 1988.

(44) Schechter, I.; Kosloff, R.; Levine, R. D. *J. Phys. Chem.* **1986**, *90*, 1006.

(45) Tsukiyama, K.; Katz, B.; Bersohn, R. *J. Chem. Phys.* **1986**, *84*, 1934. Gerlach-Meyer, U.; Kleinermanns, K.; Linnebach, E.; Wolfrum, J. *J. Chem. Phys.* **1987**, *86*, 3047.

(46) Mladenovic, M.; Zhao, M.; Truhlar, D. G.; Schenke, D. W.; Sun, Y.; Kouri, D. J. *Chem. Phys. Lett.* **1988**, *146*, 358. Truhlar, D. G. *Resonances*; ACS Symp. Ser. 263; American Chemical Society: Washington, DC, 1984.

(47) Zande, W. J. v. d.; Zhang, R.; Zare, R. N. *Spectral Line Shapes*; American Institute of Physics: New York, 1990; Vol. 6.

(48) Gerrity, D. P.; Valentini, J. J. *J. Chem. Phys.* **1983**, *81*, 1298. Veirs, D. K.; Rosenblatt, G. M.; Valentini, J. J. *J. Chem. Phys.* **1985**, *83*, 1605. *J. Chem. Phys.* **1985**, *83*, 1605. Phillips, D. L.; Levene, H. B.; Valentini, J. J. *J. Chem. Phys.* **1989**, *90*, 1600. Marinero, E.; Rettner, C. T.; Zare, R. N. *J. Chem. Phys.* **1984**, *80*, 4142. Rinnen, K. D.; Kliner, D. A. V.; Zare, R. N. *J. Chem. Phys.* **1989**, *90*, 7514.

(49) Blais, N. C.; Truhlar, D. G. *Chem. Phys. Lett.* **1983**, *102*, 120; *J. Chem. Phys.* **1985**, *83*, 2201.

(50) Bibler, N. E.; Firestone, R. F. *J. Phys. Chem.* **1972**, *76*, 621.